IDENTIFICATION OF NOVEL SCAFFOLD AS INHIBITORS OFMITOCHONDRIAL PROSTAGLANDIN E SYNTHASE (MPGES)– I

Swethan Babu R[1], Senthilkumar Palaniappan[2], M. K. Kathiravan[3]*

Abstract

Cancer is the second leading cause of death globally and around 1 in 6 patients die with an estimated case of about 28.4 million in 2040. The lower survival rate in many of the cancer cases is due to the overexpression of COX-2 and mPGES-1 through COX/mPGES-1/PGE2 pathway. The use of COX inhibitors in clinical practice today has severe side effects in the gastrointestinal, cardiovascular systems and generally decreases the formation of prostanoids like PGE2, which are necessary for fundamental cellular processes. Hence, mPGES-1 would be a more effective and safer target. In this work, a virtual screening strategy involving ligand as well as structure-based design were employed to screen a wide array of diversified chemical compounds as a basic point to identify a potential molecule as inhibitor of mPGES-1 from the readily available commercial chemical database. LY3023703 an amino imidazole derivative a selective potent inhibitor of mPGES1 was used as a query molecule. The structurally similar compounds to this inhibitor were identified through virtual screening followed by molecular docking. The top 20 molecules showed a docking score range from -7.097 to -1.776. These molecules inhibited the same binding site as Indole 2-carboxylic acid and formed key amino acid interactions, in particular, most of the ligands showed interaction with Thr131 and His53. Following this two of the potent molecules were subjected to molecular dynamics studies for 100ns and their derivatives were chosen based on synthetic feasibility and characterized. The selective screening of mPGES-1 inhibitors for inflammation and various tumor types, would open new doors and might become a novel therapeutic strategy against cancer.

Keywords: Cancer, mPGES-1 inhibitors, PGE$_2$, Virtual screening, Docking, Molecular dynamics.

[1]Department of Pharmaceutical Chemistry, SRM College of Pharmacy, SRM IST Kattankulathur,Chengalpattu, Tamil Nadu, 603203, India.

[2]Faculty of Pharmacy, Karpagam Academy of Higher Education, Pollachi Main Road, Eachanari Post, Coimbatore - 641 021, Tamil Nadu, India.

[3]*209, Dr APJ Abdul Kalam Research Lab, SRM College of Pharmacy, SRM IST Kattankulathur,Chengalpattu, Tamil Nadu, 603203, India.

***Corresponding author:** - M. K. Kathiravan
209, Dr APJ Abdul Kalam Research Lab, SRM College of Pharmacy, SRM IST Kattankulathur,Chengalpattu, Tamil Nadu, 603203, India, Email: drmkkathir@gmail.com

INTRODUCTION

Cancer is an abnormal uncontrolled proliferation of cells leading to a life-threatening disease, which can invade/spread throughout the body by different mechanisms and pathways in either sex for all age group. According to WHO, cancer is the second leading cause of death globally and around 1 in 6 patients die due to cancer with estimated cases to be 28.4 million in 2040 **[1].** According to Globocan report and pharmacoepidemiological statistics, India alone reports breast cancer (14%), lip, oral cavity cancer (10.4%), cervix cancer (8.4%), lung cancer (5.9%), stomach cancer (5%) and other cancers (56.4%) **[2].** the most common treatment procedure for cancer includes surgery, radiotherapy, and chemotherapy, whereas targeted therapies and immunotherapies are nowadays receiving more attention.

In most of the cancer forms, Inflammation is well correlated at all phases of cancer growth and malignant development **[3–5].** Chronic inflammation leads to immunosuppression which further creates a microenvironment perfect for

tumorigenesis followed by metastasis **[6].** Prostaglandins (PGs) are lipid mediators derived from 20-carbon chain fatty acid arachidonic acid (AA) which are metabolized through the cyclooxygenase pathway. AA is released from fatty acid by phospholipase A$_2$ (PLA$_2$) in the cell membrane and then transformed to PGH$_2$ in the presence of COX-1/COX-2 leading to the formation of bioactive lipids such as PGD$_2$, PGI$_2$, PGE$_2$, PGF$_2$ and TxA$_2$ (thromboxane) with the help of specific terminal enzymes **(Figure 1).** These

generated lipids have the key responsibility for the maintenance of local homeostasis of the body, act as a potent vasodilator and inhibit platelet aggregation **[7].** Among all the prostaglandins PGE_2 is abundant and

regulates physiological functions as well as pathological pathways like inflammation, fever, pain and even cancer **[8].** The PGE_2 biosynthesis involves three enzymes namely microsomal PGE synthase (mPGES)-1 and -2, and cytosolic PGE synthase (cPGES) metabolizing PGH_2 **[9, 10].**
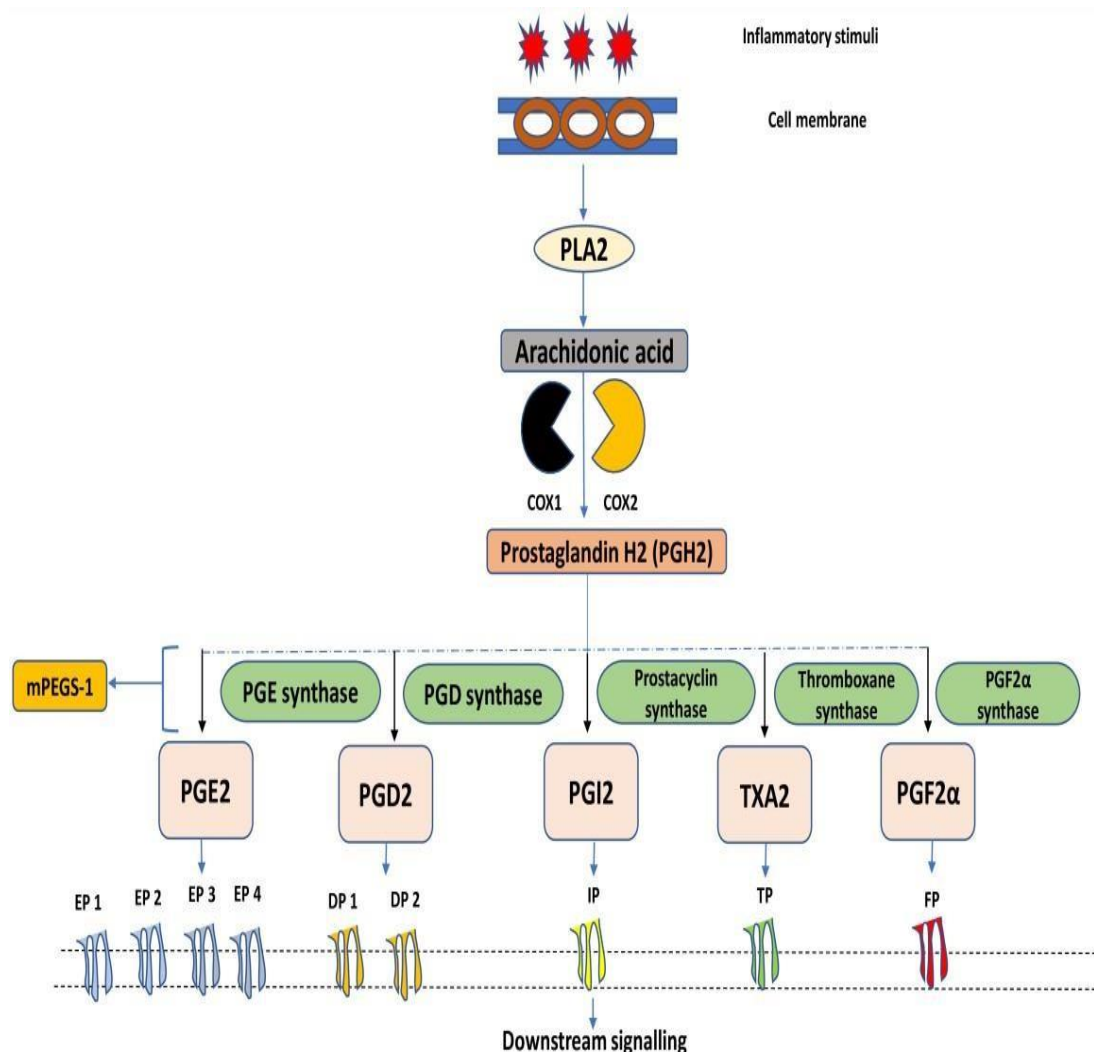

Fig.1: Overview of prostaglandin biosynthetic pathway starting from arachidonic acid

mPGES-1 is glutathione-dependent existing in microsomal membrane with a molecular weight of about 16 KDa, possessing 152 amino acids, responsible for the formation of PGE_2 during the process of inflammation. Several studies revealed that mPGES-1 is over-expressed in colon, lung, head, neck, breast, and stomach cancers **[11].** mPGES-1 is a potent target regulator of PGE_2 which is over produced when mPGES-1 is coupled with COX-2 during inflammation **[12,13].**

Furthermore, it is identified that the mPGES-2 is essentially expressed in various cell types, including human embryonic kidney cells (HEK293), human colon adenocarcinoma cells (HCA-7) and human lung epithelial cells (BEAS-2B) etc **[14,15].** There are four diverse EP receptors 1-4 that are triggered by PGE_2 which are involved in intracellular signaling pathways **[16-21].** Stimulation of tumor growth is produced by growth factors and angiogenic factors, due to the

Eur. Chem. Bull. **2023**, *12(Issue 9), 82 - 101*

83

pro-inflammatory activity of PGE_2 **[22 -24].** Recent studies have reported that few types of cancer such as neuroblastoma possess an immunosuppressive microenvironment with pro-inflammatory features. The tumor-derived PGE_2 secretion influences the production of cytokines and chemokines such as IL-6, CXCL1, G-CSF, which are known cancer-sustaining factors. These factors are produced through myeloid cells, which polarize macrophages to an M2 activation state leading to the promotion of immune evasion **[25-28].**

Literature reports that **[8,16] [23]** one of the efficient ways to reduce PGE2 production is selectively inhibiting downstream mPGES-1, which is considered to be the most effective, safer and valid target to counter various types of cancers **[29-35].** Kurtova et al. reported that the cytotoxic treatment-induced apoptosis in which the PGE_2 release promotes cancer stem cell repopulation and chemoresistance. Studies showed that the inhibition of PGE_2 with celecoxib at 5 mg/kg/day dose for two days before the combination of gemcitabine/cisplatin in treatment reduced chemotherapy resistance when the same

combination was given alone without PGE_2 inhibition in bladder cancer xenograft model **[26].** Scientific reports also point to PGE_2 suppression as a potential therapeutic approach to improve the effectiveness of immune-based therapies **[35-38].** Without altering other PGs and thromboxane, mPGES-1 can reduce PGE2 production with fewer side effects. Targeting mPGES-1 enzyme responsible for the PGE_2 synthesis will be the selective choice and will indicate newer and safe therapeutic strategies. **Figure 2** represents the list of mPGES-1 inhibitors from diverse scaffold. LY3023703 is an amino imidazole derivative discovered by Eli Lilly as a selective potent inhibitor of mPGES1. In contrast to celecoxib, which decreased inducible PGE2 production by only 44%, were as LY3023703 showed a peak increase in prostacyclin synthesis by 115% dose-dependently. The query molecule's salt form demonstrated quicker absorption than the free base and led to greater plasma concentrations. This initial success led the molecule to enter clinical trials for a single ascending dose study and multiple ascending dose studies in 48 healthy subjects for 28 days.
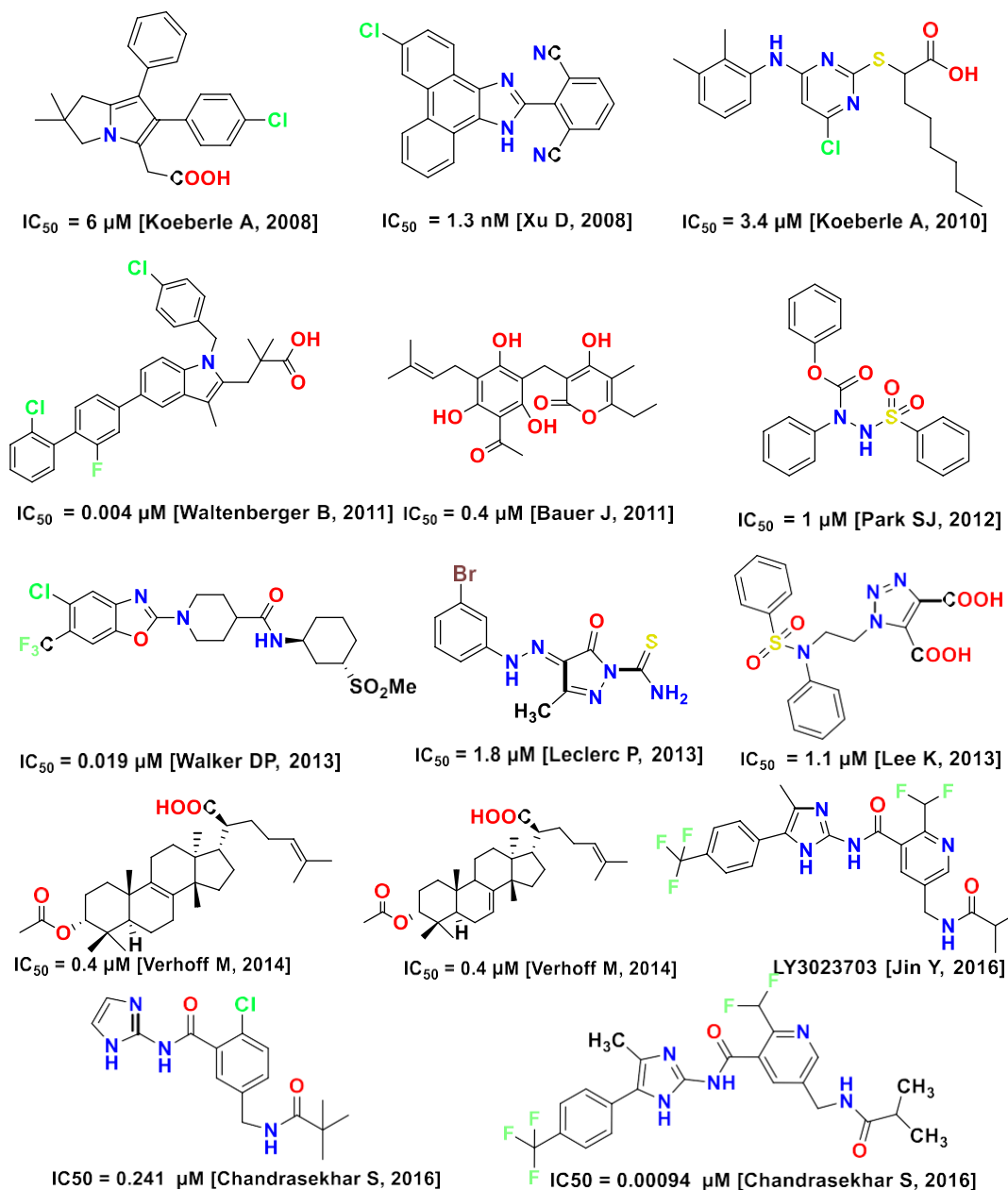
Fig.2: List of chemically diversified mPGES-1 inhibitors with IC_{50} values

However, on day 28th study, one of the trial participants experienced a considerable increase in serum aminotransferase levels, which was found to be a serious adverse event indicative of liver toxicity which led to the discontinuation of lumiracoxib. This increase in alanine aminotransferase in the phase 1 study resulted in the termination of LY3023703 for further clinical development. It was later proposed by Norman et al that LY3023703 (**Figure 3**) undergoes a key metabolic route i.e., imidazole ring epoxidation resulting in drug-induced liver damage (DILI). However, this query molecule is as a good lead due to its potent activity. Similarity search is one of the key successful strategies used in the virtual screening methodology. It is a screening technique that works by comparing the features of the potent compound with the features of each compound in the large array of the structurally diverse compound database. Hence the objective of our study was to identify a structurally similar molecule related to LY3023703 as it had the potency to be developed into a drug molecule. The query molecule amino imidazole derivative was taken as a basic scaffold and looked for similarity search in the enamine database through various filters. The scaffold similar to the query molecule will be identified as HITs which will be followed by molecular docking, molecular simulation studies and wet lab work.
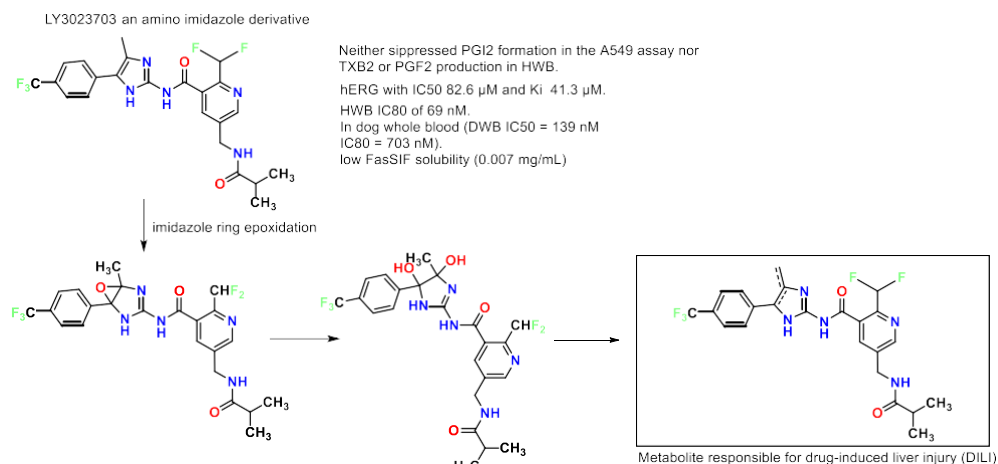
Fig.3: LY3023703 - amino imidazole derivatives metabolite shows drug induced liver injury

EXPERIMENTAL

Enamine Database

Readily Available (REAL) database is a collection of 8.5 million compounds from Enamine one of the largest commercial suppliers of chemicals. The compounds are complying with the Lipinski "rule of 5" and Veber criteria with molecular weight < 500, SlogP < 5, hydrogen bond acceptor (HBA) < 10, hydrogen bond donor (HBD) < 5, rotatable bonds < 10 and total polar surface area (TPSA) < 140. Additionally, the molecules were in a Diverse REAL drug-like dataset to avoid compounds that are toxic and PAINS. Compounds that lack analogs with Tanimoto similarity greater than 0.6 (Morgan 2 fingerprint, 512 bit) are found in the diverse REAL drug-like dataset as well as in the Enamine stock screening chemical collection.

Similarity Search using MOE

Similarity search implemented in MOE is based on generating a precise fingerprint for the molecules and calculating the similarity according to a specific threshold using a specific measuring metric. This metric can be measured and, in this study, we have applied the Tanimoto coefficient. Tanimoto coefficient is a type of symmetric similarity metric that is calculated using fingerprints in a bit form and is defined as:

$$TC(A,B) = \frac{c}{a + b - c}$$

where A and B are the two molecules to measure their similarity regarding each other, 'a' and 'b' is the fingerprint features, represented in bits, in molecule A and molecule B respectively while c is the common features fingerprints bits between molecule A and molecule B. The result of Tanimoto coefficient ranges between 0 and 1, where 0 means that the molecules are not similar since there are no common fingerprints shared between them while by increasing the value, the similarity increases and the value of 1 means that the molecules are similar and that the two molecules have identical fingerprints. Basically, the concept of using a specific fingerprint and calculating the Tanimoto coefficient is the quite often used method applied in this study. The steps involved in the similarity search using MOE is depicted in **Figure 4.** BIT MACCS fingerprints were generated for all the ligands then the similarity search process is done. Following this, the similarity is calculated using the Tanimoto coefficient for both processes independently, with setting the overlap similarity threshold to 75%.
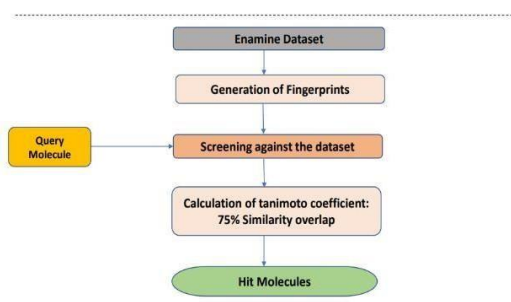

Fig.4: Mechanism for identification of Hit molecule and workflow of similarity search process from enamine database in search of mPGES-1 inhibitor

Molecular docking

The hit compounds from the similarity search were molecular docked using Schrodinger Inc.'s Glide docking software. Ligand structure and protein preparation were done as per our reported methods. The molecules were docked using the Glide docking module implemented in the Schrodinger package and the crystal structure with PDB Id: 4YL1 was selected. The 306 molecules were prepared using the ligprep module. The structure obtained from Protein Data Bank is a single monomer, however, the mPGES-1 is a homomeric trimer. The enzyme was prepared using a protein preparation wizard where the amino acid residues were optimized. After the protein preparation wizard application, the prepared enzyme is then used in Grid generation. The co-crystallized ligand Indole 2-carboxylic acid is considered the binding site and a grid is generated around the binding site for docking the ligands. Then the prepared trimer is subjected to molecular docking studies using the Glide docking tool from Schrodinger.

- **Ligand preparation:** In order to prepare high-quality, all-atom 3D structures for large numbers of drug-like molecules, starting with the 3D structures in SD Maestro format, LigPrep was used. LigPrep produced single, low-energy, 3D structures with corrected chiralities for each successfully processed input structure.
- **Preparation of protein:** The structure file from the PDB is not suitable for immediate use in molecular modelling calculations. A typical PDB structure file consists only of heavy atoms and may include a co-crystallized ligand, water molecules, metal ions, cofactors. PDB structures may be missing information on connectivity, which must be assigned, along with bond orders and formal charges. This was done using the Protein Preparation Wizard.
- **Receptor Grid Generation:** Receptor grid generation requires a "prepared" structure: an all-atom structure with appropriate bond orders and formal charges. Glide searches for favorable interactions between one or more ligand molecules and a receptor molecule, usually a protein. The shape and properties of the receptor are represented on a grid by several different sets of fields that provide progressively more accurate scoring of the ligand poses. The options in each tab of the Receptor Grid Generation panel allow defining the receptor structure by excluding any co-crystallized ligand that may be present, determine the position and size of the active site as it will be represented by receptor grids, and set up Glide constraints.

- **Ligand Docking:** The docking studies were performed using Glide Dock from Schrodinger. Glide searches for favorable interactions between one or more ligand molecules and a receptor molecule, usually a protein. Each ligand acts as single molecule, while the receptor may include more than one molecule, e.g., a protein and a cofactor. Glide was run in rigid or flexible docking modes; the latter automatically generated conformations for each input ligand. The combination of position and orientation of a ligand relative to the receptor, along with its conformation in flexible docking, is referred to as a ligand pose. The ligand poses that Glide generates pass through a series of hierarchical filters that evaluate the ligand's interaction with the receptor. The initial filters test the spatial fit of the ligand to the defined active site and examine the complementarity of ligand-receptor interactions using a grid-based method patterned after the empirical ChemScore function. Poses that passed these initial screens entered the final stage of the algorithm, which involves evaluation and minimization of a grid approximation to the OPLS-AA non bonded ligand-receptor interaction energy. Final scoring is then carried out on the energy minimized poses.

Glide Extra-Precision Mode (XP): The extra-precision (XP) mode of Glide combines a powerful sampling protocol with the use of a custom scoring function designed to identify ligand poses that would be expected to have unfavorable energies, based on well-known principles of physical chemistry. The presumption is that only active compounds will have available poses that avoid these penalties and also receive favorable scores for appropriate hydrophobic contact between the protein and the ligand, hydrogen binding interactions, and so on. The important purpose of the XP method are to eliminate false positives and to provide a better correlation between good poses and good scores. Extra-precision mod is a refinement tool designed for use only on good ligand poses. Finally, the minimized poses are re-scored using Schrodinger's proprietary Glide Score scoring function. Glide Score is based on ChemScore, but includes a steric-clash term and adds buried polar terms devised by Schrodinger to penalize electrostatic mismatches.

Molecular dynamics

The apo protein and selected protein-ligand complexes were prepared using the Solution Builder module implemented in CHARMM-GUI [39,40]. The complexes were prepared and the

Eur. Chem. Bull. **2023**, *12(Issue 9), 82 - 101*

87

simulations were performed as described before in **[41-44]**. The complexes were embedded in a 2-oleoyl-1-palmitoyl-sn-glycero-3-phosphocholine (POPC) lipid bilayer according to the suggested orientation reported in the Orientations of Proteins in Membranes (OPM) database for the template structure (PDB 4YL3) **[45].** The complexes were solvated with a rectangular box of transferable intermolecular potential with 3 points (TIP3) water molecules. In the next step, the complexes were neutralized by adding Na^+/Cl^- ions to a final concentration of 0.15M using the monte-carlo ion placing method. The ligand molecules were parameterized using the ParamChem service implemented in CHARMM-GUI. The simulation of the complexes wascarried out using CHARMM36/CGenFF (3.0.1) force fields **[46]** for protein and ligand atoms and performed under periodic boundary conditions using the Particle-Mesh Ewald method **[47]** for long-range electrostatic interactions whose grid parameters for fast Fourier transforms were determined automatically. The mPGES consists of three chains and the ligand bind to each of the chains along with the cofactor GSH. For our analysis in the study, we considered one ligand binding in the pocket. The prepared complexes from CHARMM-GUI were equilibrated over 5 ns and subjected to 100 ns of unrestrained MD simulations runs for each protein-ligand complex using NAMD. The stability of MD trajectories was analyzed by RMSD and RMSF for the protein-ligand complexes by using the RMSD trajectory tool implemented in VMD (Version 1.9.3)**[48].**

RESULTS AND DISCUSSION
Query Molecule
LY3023703 an amino imidazole derivative discovered by Eli Lilly as a selective potent inhibitor of mPGES1 and found to be 17-fold more potent than celecoxib. However, the compounds had low solubility and hence their phosphate salt was studied with a PO dose of 60 mg/kg for *in vivo* to know the Pharmacokinetics in the beagle dog. This initial success led the molecule to enter clinical trials for single incremental dose study **[49,51]** and multiple incremental dose studies in 48 healthy subjects for 28 days. The molecule had a maximum tolerated dose (MTD) as 15 mg per day or less. In comparison to celecoxib's impact (82% inhibition), LY3023703 decreased ex vivo LPS-stimulated PGE2 production by 91% and 97% on days 1 and 28, respectively. In contrast to celecoxib, which decreased inducible PGE2 production by 44%, LY3023703 showed a peak increase in prostacyclin synthesis of 115%.
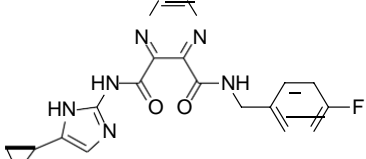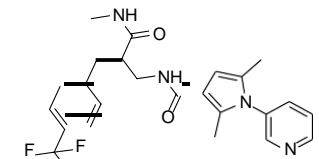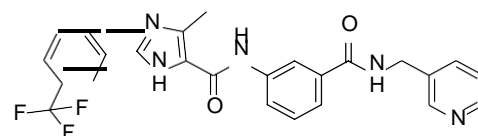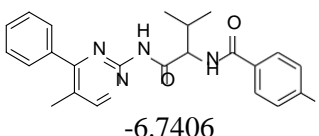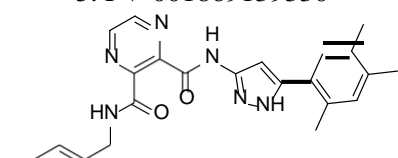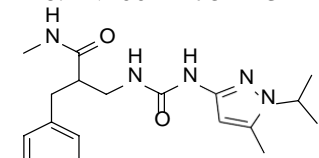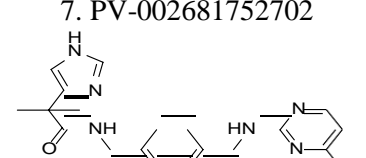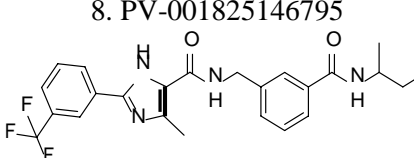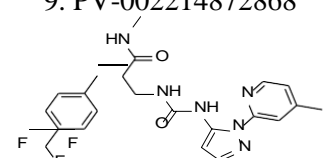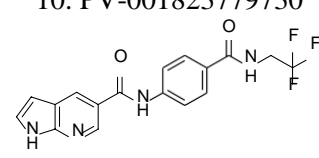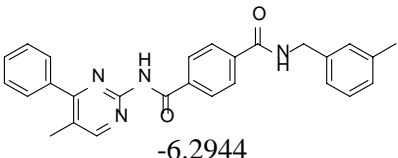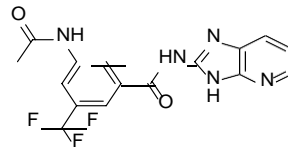
Further, the study suggests that mPGES1 is a potential target for inflammatory pain since it suppresses inducible PGE production without reducing prostacyclin formation and did not increase TXB2 formation in serum.Hence this molecule was identified as a potential lead and explored for similar structures in the available database.

Similarity search
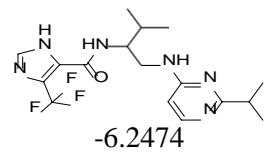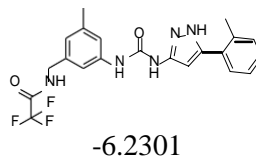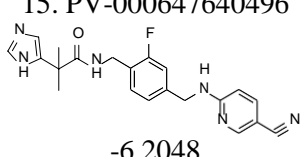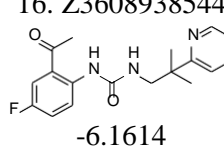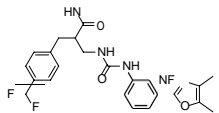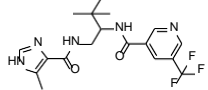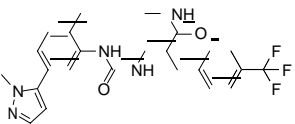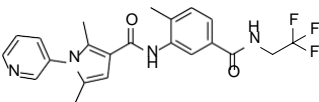The term "similarity search" refers to find a structure that is closely related to a query molecule and that is closest in a multidimensional space. The goal of this study is to perform a similarity search by screening the Enamine database of 8.5 million compounds using the query molecule to get structurally similar compounds with an aim to have an equipotent activity that can inhibit mPGES. Millions of compounds, originating from different sources in medicinal chemistry, were present in the screening database. The creation of a screening database was driven by the fact that compounds with varying bioactivities and structurally diverse scaffolds are often more challenging to separate from one another in search calculations from a random selection of bioactive heterocycles. According to the "Similar Property Principle," compounds that are structurally related to active molecules are more likely to be active themselves. Thus, finding molecules that are structurally similar to a known active molecule is one of the key methods for successful drug discovery.

First, similarity searching was applied in which 2D fingerprint 'MACCS' was calculated for our selected query molecule shown in **Figure 3** and systematically compared to compounds from Enamine Database via MOE software **[52].** Each query-target pair had a specific similarity threshold at which the agonist showed number of hits. Fingerprint overlap is quantified as a measure of molecular similarity using similarity coefficient 'Tanimoto coefficient' which is the most popular way to measure the similarity of molecular fingerprints. For our similarity search we selected the threshold value of 75 % similarity overlap. The search against the Enamine Database has resulted 306 molecules as hits. When the threshold value was increased to 80% the number of hit molecules is reduced from 306 to 20. This showed that high number of molecules was identified as hits within the range from 75 to 80% similarity overlap. The highly similar 20 molecules were shown in **Table 1**. However, for our docking calculation we considered all the 306 molecules **[53, 54].**

Eur. Chem. Bull. **2023**, *12(Issue 9), 82 - 101*

88

Table 1. Hit Molecules Identified Using Similarity Search With The Threshold Of 80% Similarity Overlap Along With Its Dock Score.

1. PV-001857177657	2. PV-002331049037
-7.0968	-7.0118
3. PV-002362919606	4. PV-002562830538
-6.8185	-6.7406
5. PV-001869139330	6. PV-002147811234
-6.7180	-6.6782
7. PV-002681752702	8. PV-001825146795
-6.5635	-6.4811
9. PV-002214872868	10. PV-001823779730
-6.4245	-6.3861
11. PV-001805218556	12. Z1452910845
-6.2944	-6.2727
13. PV-002679826848	14. PV-001947172169
-6.2474	-6.2301
15. PV-000647640496	16. Z3608938544
-6.2048	-6.1614

17. PV-002475660589	18. PV-001144654165
-6.1189	-6.1052
19. Z3291026606	20. Z768814574
-6.0908	-6.0283

Molecular Docking

There are three distinct subtypes of PGES, and mPGES-1 is one of the potential targets for pain. At present 18 crystal structures for mPGES-1 are accessible in the protein data library **(Table 2)** and the structures are complexed with different potential molecule with high resolution. One of the structure belonging to phenanthrene imidazoles, MF63 that carries a 2,6-dicyano-substituted phenyl ring in 2-position of the imidazole was also a promising candidate **(Figure 5) [50].** The 2,6-dicyanophenyl group points inward and clamped between the two protein chains. One of the nitrile

group on the backside forms van der Waals contact with the Cβ of Ala123 (monomer 1) at a distance of 3.6 Å and with the side chain hydroxyl of Ser127 (monomer 1) located at a distance of 3.2 Å. The another nitrile function group fits across L39 side chain (monomer 2) and attracting water molecules in front of the binding site. However, among the crystal structures for the docking study the mPGES-1 in complex with one of the potent inhibitors Indole 2-carboxylic acid was considered and proceed for molecular docking studies.
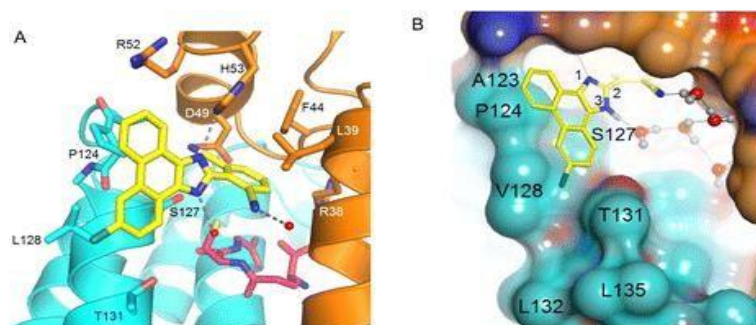
Figure 5. Crystal structure of mPGES in complex with MF63 (Luz J.G, 2015). A. Phenanthrene imidazole MF63 with the 2,6-dicyano-phenyl is buried within the binding 605 pocket B. Surface representation of Phenanthrene imidazole MF6.

Table 2: List Of Crystal Structure Available For Mpges-1

PDB ID	Protein	Species	Structure Title	Release Year	Resolution (Å)	Scaffold Name
2PBJ	mPGES	monkey	GSH-heme bound microsomal prostaglandin E synthase	2008	2.80	-
4YL3	mPGES-1	human	Crystal Structures of mPGES-1 Inhibitor Complexes	2015	1.41	Imidazopyridine
4YL1	mPGES-1	human	Crystal Structures of mPGES-1 Inhibitor Complexes	2015	1.41	Indole 2-carboxylic acid
4YL0	mPGES-1	human	Crystal Structures of mPGES-1 Inhibitor Complexes	2015	1.52	Phenanthrene imidazole

4YK5	mPGES-1	human	Crystal Structures of mPGES-1 Inhibitor Complexes	2015	1.42	Indole propionic acid
1Z9H	mPGES-2	monkey	Microsomal prostaglandin E synthase type-2	2005	2.60	-
6VL4	mPGES-1	human		2020		Phenylacetic acid
5BQI	mPGES-1	human	Discovery of a Potent and Selective mPGES-1 Inhibitor for the Treatment of Pain	2016	1.88	Pyridine 3-carboxmide
5BQH	mPGES-1	human	Discovery of a Potent and Selective mPGES-1 Inhibitor for the Treatment of Pain	2016	1.60	Benzamide
5BQG	mPGES-1	human	Crystal Structure of mPGES-1 Bound to an Inhibitor	2016	1.44	Benzamide
4AL1	mPGES-1	human	Crystal structure of Human PS-1 GSH-analog complex	2013	1.95	-
4AL0	mPGES-1	human	Crystal structure of Human PS-1	2013	1.16	-
5T37	mPGES-1	human	crystal structure of mPGES-1 bound to inhibitor	2017	1.76	Benzamide
5T36	mPGES-1	human	Crystal structure of mPGES-1 bound to inhibitor	2017	1.40	2-Amino benzoic acid
5K0I	mPGES-1	human	mpges1 bound to an inhibitor	2016	1.30	Quinoline
5TL9	mPGES-1	human	crystal structure of mPGES-1 bound to inhibitor	2017	1.20	Benzoic acid
4WAB	Fused mPGES-1 with LTC4S	human	Crystal structure of mPGES1 solved by native-SAD phasing	2014	2.70	Benzimidazole
4BPM	Fused mPGES-1 with LTC4S	human	Crystal structure of a human integral membrane enzyme	2014	2.08	Benzimidazole

The 306 molecules identified as hit molecules from similarity search using MOE were subjected to molecular docking. The docking studies were carried out with crystal structure PDB Id: 4YL1 and the docking score was obtained in the range from -7.097 to -1.776. The top 20 molecules obtained from docking studies with their docking score greater than -6.0 kcal/mol are shown in **Table 1.** However only 2 molecules had binding score of about -7 such as in compound PV-001857177657 and PV-002331049037. Remaining 18 molecules had dock score between -6.0 to -6.8. These twenty molecules includes mono atomic as well as diatomic nitrogen containing structures such as pyrazole, pyrimidine, pyrimidines, imidazole, pyrazine as well as fused pyrrolo[2,3-b]pyridine and imidazo[4,5-b]pyridine substitution. Almost all the molecules had amide substitution and many of the compounds had mono and trifluoro substitution except compound PV-001805218556. The top two molecules were selected based upon their similar binding site of Indole 2-carboxylic acid and showed similar interactions with the amino acid residues. The amino acid interactions confirms that the identified molecules are similar to the query molecule (**Figure 6**). In particular, most of the ligands form interaction with Thr131 and His53. The binding poses and the 2D interaction of the top 5 molecules in shown in **figure 6 [51 – 57].**

Eur. Chem. Bull. **2023**, *12(Issue 9), 82 - 101*

91

A)

B)

C)

Eur. Chem. Bull. **2023**, *12(Issue 9), 82 - 101*

92

D)

E)
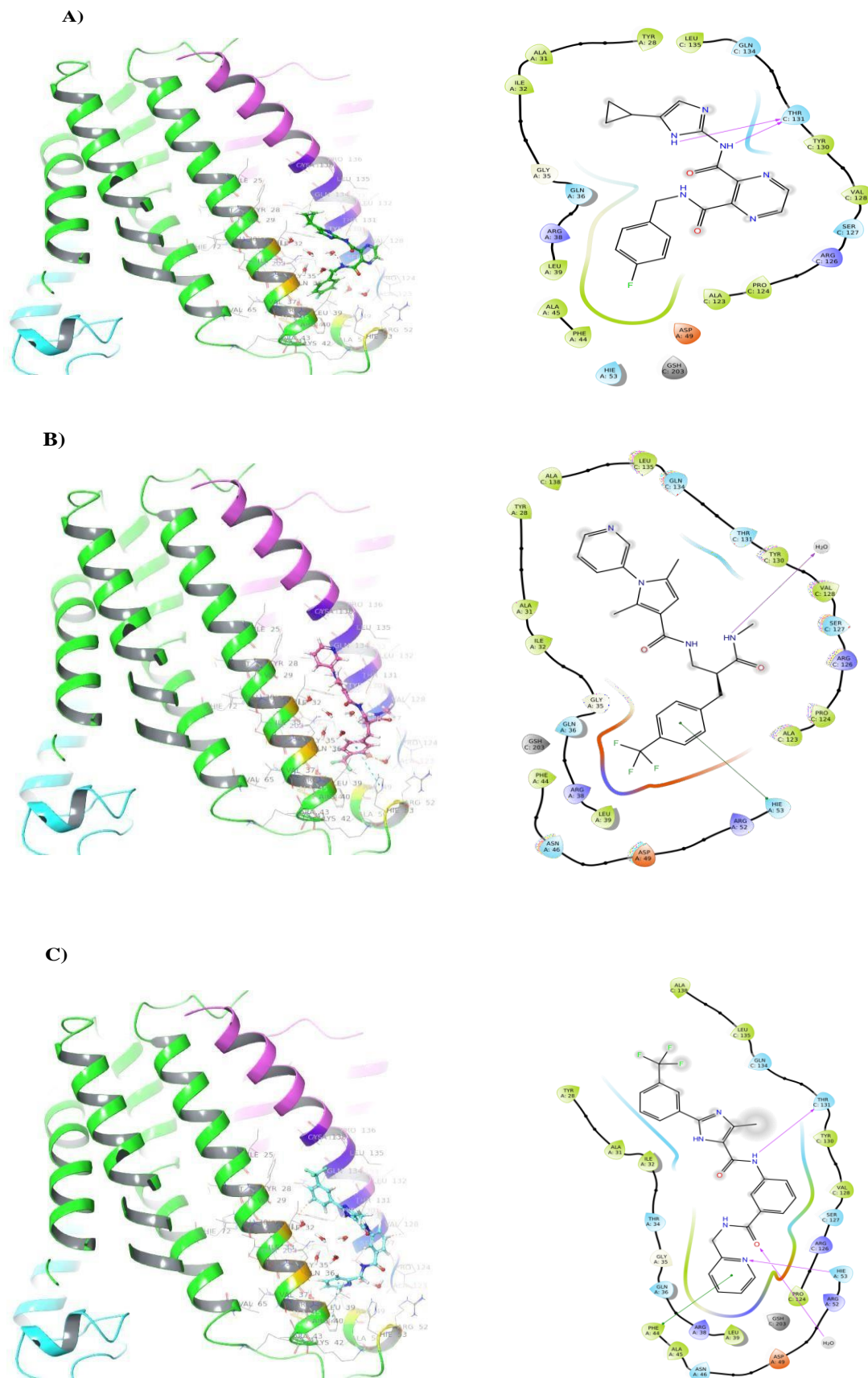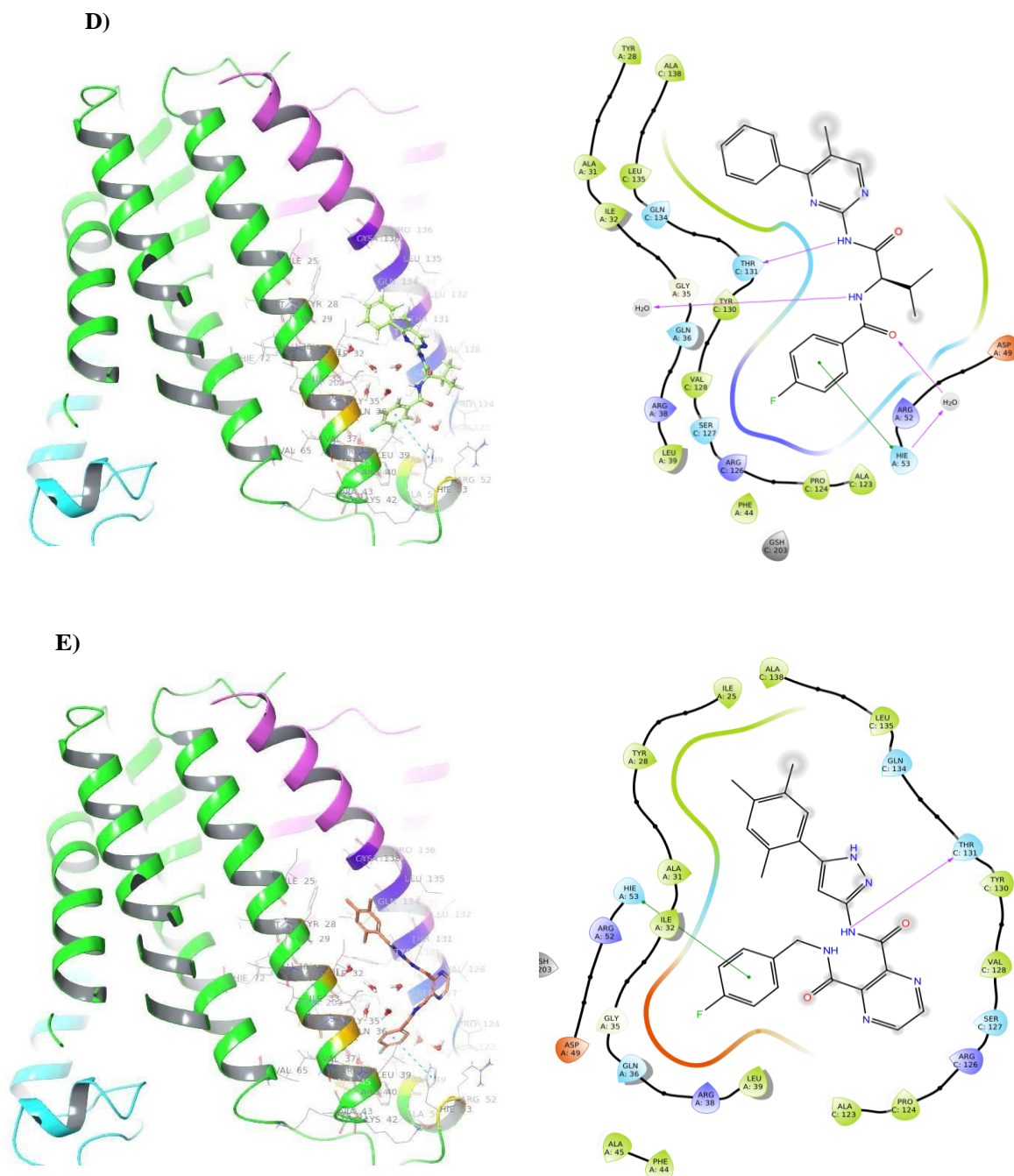
Fig.6: The binding poses of the top five molecules (A) PV-001857177657 (B) PV-002331049037 (C) PV-002362919606 (D) PV-002562830538 (E) PV-001869139330 are shown with their amino acid residues in the binding pocket and their 2D interaction diagrams.

ADMET Studies

Drug-likeness properties of these 20 compounds were studied by employing in silico studies 'Adsorption, distribution, metabolism, elimination and toxicity' analysis. In silico ADMET prediction for the target compounds were carried out in early stage to reduce the risk. The pharmacokinetic profiles of the molecules were predicted using Osiris property explorer. Off all the verified molecules only PV-001869139330 showed toxicity characteristics properties **(Table 3).**

Eur. Chem. Bull. **2023**, *12(Issue 9), 82 - 101*

93

Table 3: Predictive Properties Calculated Using Osiris Property Explorer

S.no	Hit molecules	Dock score	log P	log S	TPSA Å	Drug likeness	HBA	HBD	Number of Stereo-centers	Number of rotatable bonds	Drug-Score	Mutagenic	Tumorigenic	Irritant	Reproductive Effective
1	PV-001857177657	-7.0968	1.57	-3.29	112.66	3.46	8	3	0	6	0.88	In-Act	In-Act	In-Act	In-Act
2	PV-002331049037	-7.0118	3.12	-5.99	76.02	-1.35	6	2	1	8	0.46	In-Act	In-Act	In-Act	In-Act
3	PV-002362919606	-6.8185	3.77	-5.79	99.77	-4.19	7	3	0	7	0.35	In-Act	In-Act	In-Act	In-Act
4	PV-002562830538	-6.7406	3.92	-5.41	83.98	3.38	6	2	1	6	0.75	In-Act	In-Act	In-Act	In-Act
5	PV-001869139330	-6.7180	2.90	-5.14	112.66	2.31	8	3	0	6	0.47	Act	Act	In-Act	In-Act
6	PV-002147811234	-6.6782	2.69	-3.83	88.05	-0.52	7	3	1	8	0.56	In-Act	In-Act	In-Act	In-Act
7	PV-002681752702	-6.5635	1.80	-3.91	104.82	1.51	8	3	0	8	0.79	In-Act	In-Act	In-Act	In-Act
8	PV-001825146795	-6.4811	4.28	-6.03	86.88	-3.34	6	3	1	8	0.35	In-Act	In-Act	In-Act	In-Act
9	PV-002214872868	-6.4245	3.84	-3.54	100.94	-0.60	8	3	1	8	0.47	In-Act	In-Act	In-Act	In-Act
10	PV-001823779730	-6.3861	2.64	-4.75	86.88	-4.76	6	6	0	5	0.45	In-Act	In-Act	In-Act	In-Act
11	PV-001805218556	-6.2944	4.91	-6.19	83.98	-3.29	6	2	0	6	0.33	In-Act	In-Act	In-Act	In-Act
12	Z1452910845	-6.2727	2.61	-4.78	99.77	-14.75	7	3	0	4	0.44	In-Act	In-Act	In-Act	In-Act
13	PV-002679826848	-6.2474	2.25	-3.04	95.59	-3.27	7	3	1	8	0.45	In-Act	In-Act	In-Act	In-Act
14	PV-001947172169	-6.2301	3.38	-6.11	98.91	-25.92	7	4	0	6	0.39	In-Act	In-Act	In-Act	In-Act
15	PV-000647640496	-6.2048	1.90	-4.60	106.49	-2.84	7	3	0	7	0.46	In-Act	In-Act	In-Act	In-Act
16	Z3608938544	-6.1614	2.79	-4.46	71.09	-0.09	5	2	0	5	0.66	In-Act	In-Act	In-Act	In-Act
17	PV-002475660589	-6.1189	4.15	-6.58	96.26	-7.50	7	3	1	8	0.34	In-Act	In-Act	In-Act	In-Act
18	PV-001144654165	-6.1052	2.09	-3.03	99.77	-9.13	7	3	1	7	0.26	In-Act	In-Act	In-Act	In-Act
19	Z3291026606	-6.0908	3.30	-5.14	88.05	-0.30	7	3	1	8	0.52	In-Act	In-Act	In-Act	In-Act
20	Z768814574	-6.0283	3.46	-6.77	76.02	-3.27	6	2	0	6	0.40	In-Act	In-Act	In-Act	In-Act

HBA and HBD - number of hydrogen bond acceptors and donors; 'Log P - lipophilicity Log S - Solubility; TPSA - topological polar surface area (Å)'; In-Act indicates Inactive and Act indicate Active.

Molecular dynamics

To understand the stability of the ligands identified from docking studies, the top-ranked molecules PV-001857177657 and PV-002331049037 were subjected to MD simulations. In addition to the apo protein, the two protein-ligand complexes were prepared using CHARMM-GUI and MD simulation was performed for a period of 100 ns. From analyzing the generated trajectories of the complexes, the root mean square deviation (RMSD) values of the Cα atoms of the mPGES protein reached the steady state approximately within 2.0 - 3.0 Å deviations from its initial structure **(Figure 7a)**. This specifies that the mPGES protein maintains the interaction profile and does not undergo larger conformational changes upon binding of the two ligands PV-001857177657 and PV-002331049037. The visual interpretation of the trajectories showed that both ligands were anchored inside the binding pocket identified from the docking studies. The extracellular region connecting the two transmembrane regions of the protein largely controls the ligands inside the binding pocket **(Supplementary figure S1 and S2)**. This can also be visualized with root mean square fluctuation profile for the complexes with the ligands PV-001857177657 and PV-002331049037 in comparison to the apo structure of mPGES protein **(Figure 7b)**. In reference to the apo structure, the regions where the two ligands bind found structural changes and the remaining region of the protein are very similar. In comparison with ligand PV-001857177657, PV-002331049037 induces large conformation in this region. This is possibly due to the Trifluoro methyl (CF_3) functional group present in ligand PV-002331049037 compared to mono fluorine (F) of the phenyl group. The hydrogen bond interaction analysis show that the two ligands interact with Thr131 majorly in comparison to the other amino acid residues and largely bounded by hydrophobic interaction in comparison to electrostatic interactions **(Supplementary table S1)**. Additionally, to confirm the presence of ligands within the binding pocket of mPGES, the distance between the center of ligands and the cofactor GSH was analyzed across the trajectory of 100 ns **(Supplementary Figure S3)**. The distance is mostly around 6-8 Å which is comparable to the distance measured (11.2 Å) in the reference crystal structure (PDB Id: 4YL1) for the ligand, Indole 2-carboxylic acid selected in the docking study and molecular dynamics. This is further supported by the initial results from the docking studies, where major interaction are from hydrophobic residues. The molecular dynamic studies provide an understanding of the two ligands identified from molecular docking, their stability, and interactions with the residues in the binding pocket **[58-61].**
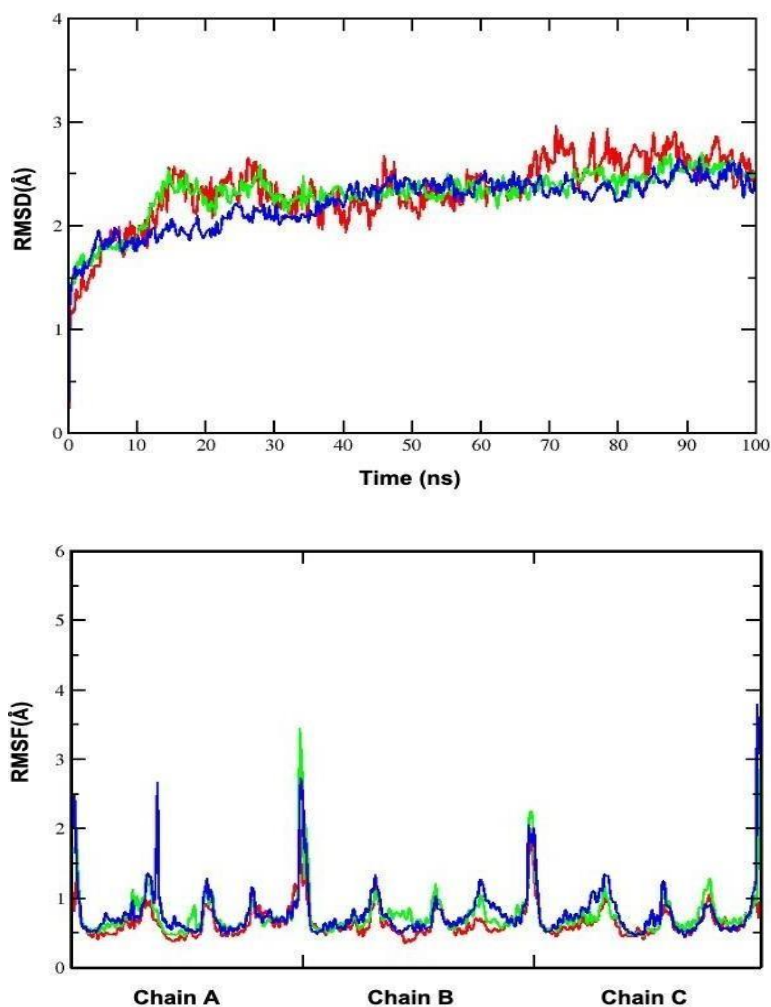
Fig.7: Molecular dynamic simulation studies of the protein-ligand complexes. A) Root mean square deviation (RMSD) values and B) Root mean square fluctuation (RMSF) obtained from the Cα atoms relative to the initial frame of the production run of 100 ns simulations for the protein-ligand complex for the selected ligands, PV-001857177657(Green), PV-002331049037(Blue) in comparison with apo protein structure (red)

Chemistry

From the theoretical studies two molecules among the top five belonging to same scaffold were subjected to laboratory synthesis **(Figure 8)**. 5-cyclopropyl-4-methyl-1H-imidazol-2-amine, was prepared by cyclization of 1-cyclopropylpropane-1,2-dione (1mmol) with formamide (1mmol) in presence glacial acetic acid and ammonium acetate. Glyoxal and *ortho*-phenylenediamine were reacted in water followed by reaction with sodium carbonate yielded compound **(2)**. Compound **2** was hydrolyzed by oxidizing with hot aqueous potassium permanganate solution and the mixture was cooled at room temperature to give potassium pyrazine-2,3-dicarboxylate **(3)**. Compound (**3**) was acidified with 36% hydrochloric acid, filtered and recrystallized with acetone to give pyrazine-2,3-dicarboxylic acid **(4)**. Furo[3,4-b]pyrazine-5,7-dione (anhydride) **(5)** was obtained by reacting pyrazine-2,3-dicarboxylic acid **(4)** with acetic

anhydride at 125° C. Compound **(6)**, 3-((5-cyclopropyl-4-methyl-1H-imidazol-2-yl) carba-moyl)pyrazine-2-carboxylic acid, was prepared from anhydride compound **(5)** in presence of Sodium dodecyl sulfate. Compound **(6)** was treated with ammonia to give N^2-(5-cyclopropyl-4-methyl-1H-imidazol-2-yl) pyrazine-2,3-dicarbo-xamide **(7)**. Compound **(7)** reacted with benzyl chloride to yield N^2-(5-cyclopropyl-4-methyl-1H-imidazol-2-yl)-N3-substitutedphenyl)-2,3dihydro pyrazine -2,3-dicarboxamide **(8)**. However a total of sixteen molecules from series 8 with a wide range of substitution such as hydrogen, methyl, methoxy, nitro, amino and dimethyl amino at 2,3,4 position and one compound from series 9 were synthesized.

The purity of the synthesized compounds was monitored by TLC and elemental analyses. All the fifteen synthesized compounds were characterized

Eur. Chem. Bull. **2023**, *12(Issue 9), 82 - 101*

95

by spectral analysis (IR, ^{1}H-NMR, ^{13}C-NMR and MS). The percentage yield of synthesized compounds in all the stages were found to be in the range of 65 and 73%. IR spectra of compounds confirmed the presence of –NH, and –N=C in the imidazole ring by stretching bands at 3332, 1551 cm^{-1} respectively. Presence of amide (-NHCO) confirmed by stretching band at 1660 cm^{-1}. Proton assignments in ^{1}H-NMR spectra for the compounds showed signal at δ 11.5-11.7 (s, NH imidazole), δ 9.2-9.3 (b*s*, 2NH- amide), δ 7.4-7.6 (*m*, Ar-H imidazole & pyrazine), δ 6.9-7.3 (*m*, Ar-H), 3.2-3.3 (*s*, -CH$_3$), δ 3.0 (*d*, 2CH$_2$ pyrazine), δ 2.7-2.8 (*d*, 2CH$_2$ cyclopropane), and δ 1.9 (*s*, CH

cyclopropane),. The compounds showed a characteristic peak in the range δ 6.5-6.6 for primary amine and at δ 8.9-9.0 for phenolic OH. The spectra also confirmed the presence of the characteristic peaks corresponding to the protons attached. ^{13}C-NMR of the compounds shows characteristic peaks at δ 174.1-174.4 (CONH), 142.4-142.6 (carbonyl carbon in pyrazine ring), 07.9-8.6 (cyclopropane -CH-H$_2$C-CH$_2$). Additionally, mass spectra (m/z values) and elemental analyses (C, H, and N) both confirmed the named compounds and found them to be within 0.4% of theoretical values.
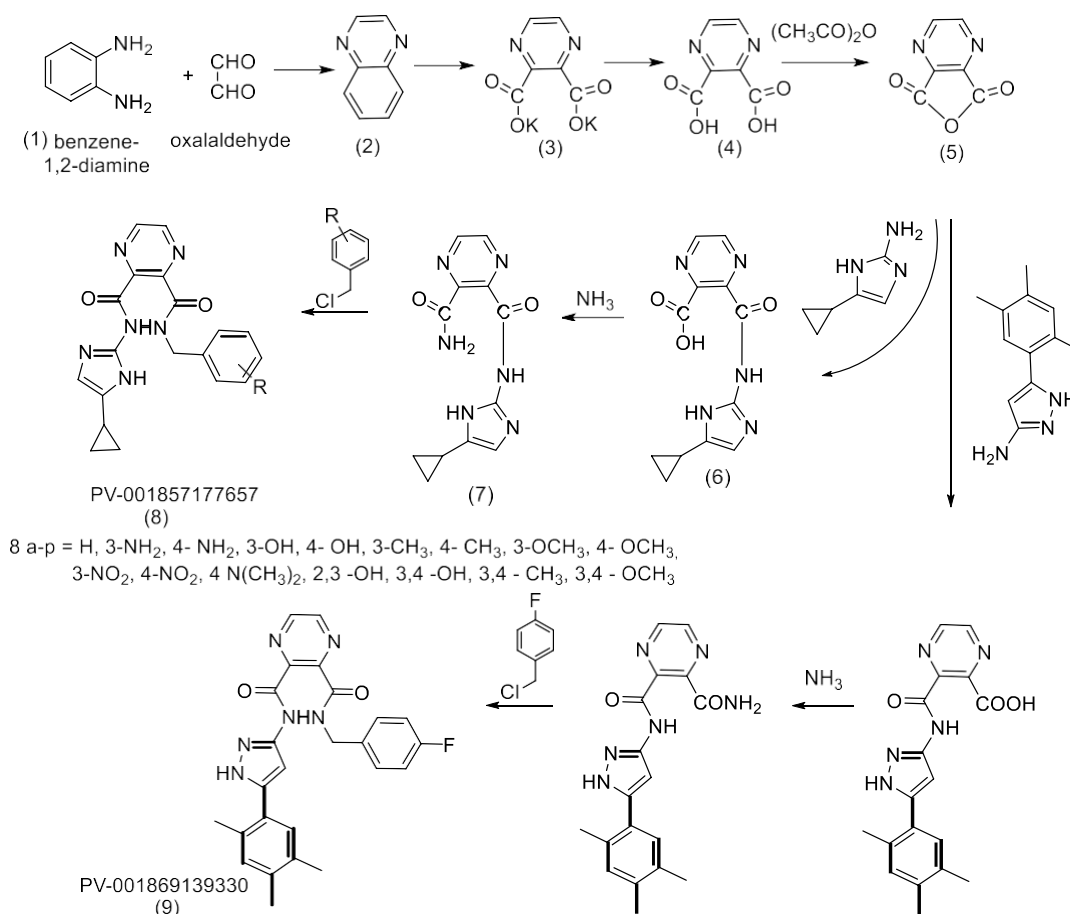

Fig.8: Synthetic Scheme for a series of derivatives from the top ligand PV-001857177657

CONCLUSION

The goal of the similarity study is to use a computational approach and identify potential molecules from a library of chemical compounds in order to find new bioactive heterocycle as potent mPGES-1 inhibitors. From the screening library of enamine database, 306 compounds were identified and subjected to molecualr docking studies with help of Glide docking tool followed by molecualr dynaics. The top poses of compounds having good protein binding affinity were selected. Hit molecules obtained using similarity approach showed a docking score range from -7.097 to -

1.776 kcal/mol. All the top 20 molecules inhibited the same binding site similar to Indole 2-carboxylic acid and formed the required interactions with the amino acid residues in the binding site, in particular most of the ligands formed interaction with Thr131 and His53. The molecular docking studies showed the insights at the atomic level interaction to understand the mechanism and binding. These molecules were chosen for synthesis, characterized and further investigation is on their biological activity. These scaffolds demonstrate that a combined ligand and structure-based virtual screening technique could potentially

Eur. Chem. Bull. **2023**, *12(Issue 9), 82 - 101*

96

discover viable candidates as potential molecules for mPGES-1 against cancer. It can be concluded that the amide linker (-CONH-) attached to the pyrazole as well as imidazole plays a key interaction with the protein, is responsible for the biological activity with more selective and have tight binding affinity than the other molecules. The MD simulation and analysis of the trajectories showed that the mPGES protein maintains its interaction profile upon binding to PV-001857177657 and PV-002331049037 with stable RMSD values. Furthermore, analysis with RMSF, PV-001857177657 is more stable with hydrophobic interaction with the amino acids in the binding pocket and the extracellular loop connecting the transmembrane regions. The study identified a potential molecules targeting cancer will lead and contribute for the development of new leads to over the drawback of existing molecules. Furthermore, more experiments on the biological part are under progress to identify the structural requirement for inhibition activity.

DECLARATIONS

REFERENCES
1. World Health Organization (WHO). https://www.who.int/news-room/fact-sheets/detail/cancer.
2. World Health Organization (WHO). India source: Globocan 2018. Available at: https://gco.iarc.fr/today/data/factsheets/populations/356-india-fact-sheets.pdf\
3. Sergei I Grivennikov , Florian R Greten, Michael Karin. (2010). Immunity, inflammation, and cancer. Cell, 19;140(6), 883-99. doi: 10.1016/j.cell.2010.01.025
4. Lisa M Coussens., Zena Werb. (2002). Inflammation and cancer, Nature. 19-26; 420 (6917), 860-7. doi: 10.1038/nature01322.
5. Shanthini M Crusz., Frances R Balkwill. (2015). Inflammation and cancer: advances and new agents. Nature Reviews Clinical Oncology, 12(10):584-96. doi: 10.1038/nrclinonc.2015.105.
6. Shacter, E., and Weitzman, S. A., (2002). Chronic Inflammation and cancer. Oncology (Williston park),16, 217-226, discussion, 230-212
7. Kijeong, Lee., Sang, Hag Lee., and Tae Hoon, Kim. (2020). The Biology of Prostaglandins and Their Role as a Target for Allergic Airway Disease Therapy International Journal of Molecular Sciences, 21 (5), 1851. doi:10.3390/ijms21051851
8. Yuqing Chen., Huaqing Liu., and Shuang Xu., (2015). Targeting microsomal prostaglandin E2 synthase-1 (mPGES-1): the development of inhibitors as an alternative to non-steroidal anti-inflammatory drugs (NSAIDs). Med Chem Comm., doi:10.1039/C5MD00278H
9. Santiago Zelenay., Annemarthe G van der Veen., Jan P Böttcher., Kathryn J Snelgrove., Neil Rogers., Sophie E Acton., Probir Chakravarty., Maria Romina Girotti., Richard Marais., Sergio A Quezada., Erik Sahai., Caetano Reis e Sousa. (2015). Cyclooxygenase-Dependent Tumor Growth through Evasion of Immunity. Cell, 162 (6), 1257-70.doi:10.1016/j.cell.2015.08.015
10. William L. Smith., Yoshihiro Urade., and Per-Johan Jakobsson. (2011). Enzymes of the Cyclooxygenase Pathways of Prostanoid Biosynthesis. Chemical reviews, 111(10): 5821 –5865, doi: 10.1021/cr2002992
11. Karin Larsson., Anna Kock., Per Kogner., & Per-Johan Jakobsson. (2019). Targeting the COX/mPGES-1/PGE$_2$ pathway in neuro-blastoma. Advances in Experimental Medicine and Biology, 1161, 89-100. doi:10.1007/978-3-030-21735-8_9.
12. Anastasia Psarra., Aikaterini Nikolaou., Maroula G Kokotou., Dimitris Limnios., & George kokotos. (2017). Microsomal prostaglandin E2 synthase-1 inhibitors: a patent review. Expert Opinion on Therapeutic Patents, 9, 1047-1059. doi:10.1080/13543776.2017.1344218.
13. Karin Larsson., Anna Kock., Helena Idborg.,Marie ArsenianHenriksson., Tommy Martinsson., JohnI. Johnsen., Marina Korotkova., Per Kogner., & Per-Johan Jakobsson. (2015). COX/ mPGES-1/PGE2 pathway depicts an inflammatory-dependent high-risk neuro blastoma subset. Medical sciences, 112 (26) 8070-8075. doi:10.1073/pnas.1424355112.
14. Murakami, M.; Nakashima, K.; Kamei, D.; Masuda, S.; Ishikawa, Y.; Ishii, T.; Ohmiya, Y.; Watanabe, K.; Kudo, I. (2003). Cellular prostaglandin E2 production by membrane-bound prostaglandin E synthase-2 via both cyclooxygenases-1 and -2. Journal of Biological Chemistry, 278, 37937–3794.

Eur. Chem. Bull. **2023**, *12(Issue 9), 82 - 101*

97

doi: 10.1074/jbc.M305108200

15. Gianluigi Lauro., Vincenza Cantone., Marianna Potenza., Katrin Fischer., Andreas Koeberle., Oliver Werz., Raffaele Riccio., and Giuseppe Bifulco. (2018). Discovery of 3-hydroxy-3-pyrrolin-2-one-based mPGES-1 inhibitors using a multi-step virtual screening protocol. Medchemcomm, 9, 2028–2036. doi:10.1039/c8md00497h

16. Karin Larsson., Per-Johan Jakobsson. (2015). Inhibition of microsomal prostaglandin E synthase-1 as targeted therapy in cancer treatment. Prostaglandins & Other Lipid Mediators, 120, 161-5. doi:10.1016/j.prostaglandins.2015.06.002.

17. Kijeong Lee., Sang Hag Lee., Tae Hoon Kim. (2020). The Biology of Prostaglandins and Their Role as a Target for Allergic Airway Disease Therapy. International journal of molecular sciences. 21(5), 1851, doi:10.3390/ijms21051851

18. Masako Nakanishi., Daniel W., Rosenberg., (2013). Multifaceted roles of PGE_2 in inflammation and cancer. Seminars in Immunopathology, 35(2), 123-37. doi:10.1007/s00281-012-0342-8.

19. Liu Bing., Qu Liyan., and Yan Shigui. (2015). Cyclooxygenase-2 promotes tumor growth and suppresses tumor immunity. Cancer Cell International, 5, 106. doi:10.1186/s12935-015-0260-7.

20. Brocard E., Oizel K., Lalier L., Pecqueur C., Paris F., and Vallette FM. (2015). Radiation-induced PGE_2 sustains human glioma cell growth and survival through EGF signaling. Oncotarget, 6(9), 6840-6849. doi:10.18632/oncotarget.3160

21. Kurtova AV., Xiao J., Mo Q., Pazhanisamy S., Krasnow R., and Lerner SP. (2015). Blocking PGE2-induced tumour repopulation abrogates bladder cancer chemoresistance. Nature, 517, 209-13. doi:10.1038/nature14034

22. Anna Kock., Karin Larsson., Filip Bergqvist., Nina Eissler., Lotta H.M. Elfman., Joan Raouf., Marina Korotkova., John Inge Johnsen., Per-Johan Jakobsson., Per Kogner. (2018). Inhibition of Microsomal Prostaglandin E Synthase-1 in Cancer-Associated Fibroblasts Suppresses Neuroblastoma Tumor Growth. eBioMedicine, 32, 84-92. doi:10.1016/j.ebiom.2018.05.008

23. Filip Bergqvist., Ralf Morgenstern., Per-Johan Jakobsson. (2020). A review on mPGES-1 inhibitors: From preclinical studies to clinical applications. Prostaglandins Other Lipid Mediators, 147, 106383.

doi:10.1016/j.prostaglandins.2019.106383

24. Wang Dingzhi., Dubois Raymond N. (2010). Eicosanoids and cancer. Nature Reviews Cancer, 10, 181-93. doi:10.1038/nrc2809.

25. Valentina Comunanza., (2018). Targeting mPGES-1 as a New strategy against Neuroblastoma. eBioMedicine, 33, 14-15. doi:10.1016/j.ebiom.2018.06.008.

26. Santiago Zelenay., Annemarthe G van der Veen., Jan P Böttcher., Kathryn J Snelgrove., Neil Rogers., Sophie E Acton., Probir Chakravarty., Maria Romina Girotti., Richard Marais., Sergio A Quezada., Erik Sahai., Caetano Reis e Sousa. (2015). Cyclo-oxygenase-Dependent Tumor Growth through Evasion of Immunity. Cell, 162(6), 1257-1270. doi:10.1016/j.cell.2015.08.015.

27. David G.Menter., and Raymond N. DuBois. (2012). Prostaglandins in Cancer Cell Adhesion, Migration, and Invasion. International Journal of Cell Biology, 1-21. doi:10.1155/2012/723419.

28. Andreas Koeberle., Stefan A. Laufer., and Oliver Werz. (2016). Design and Development of Microsomal Prostaglandin E2 Synthase-1 Inhibitors: Challenges and Future Directions. Journal of Medicinal Chemistry, 59, (13), 5970–598. doi:10.1021/acs.jmedchem.5b01750.

29. Bahadır Bülbül., İlkay Küçükgüzel. (2019). Microsomal Prostaglandin E2 Synthase-1 as a New Macromolecular Drug Target in the Prevention of Inflammation and Cancer. Anticancer Agents in Medicinal Chemistry, 19 (10), 1205-1222. doi:10.2174/1871520619666190227174137.

30. Yuka Sasaki., Yoshihito Nakatani., Shuntaro Hara. (2015). Role of microsomal prostaglandin E synthase-1 (mPGES-1)-derived prostaglandin E2 in colon carcinogenesis. Prostaglandins &Other Lipid Mediators, 121, 42-45.

doi:10.1016/j.prostaglandins.2015.06.006.

31. Suhaib Shekfeh., Burcu Çalışkan., Katrin Fischer., Tansu Yalçın., Dr. Ulrike Garscha., Prof. Oliver Werz., Prof. Erden Banoglu. (2018). A Multi-step Virtual Screening Protocol for the Identification of Novel Non-acidic Microsomal Prostaglandin E2 Synthase-1 (mPGES-1) Inhibitors. ChemMedChem, 14, 273-281. doi:10.1002/cmdc.201800701.

32. Gianluigi Lauro., Michele Manfra., Silvana Pedatella., Katrin Fischer., Vincenza Cantone., Stefania Terracciano., Alessia Bertamino., Carmine Ostacolo., Isabel Gomez-Monterrey., Mauro De Nisco., Raffaele Riccio., Ettore

Eur. Chem. Bull. **2023**, *12(Issue 9), 82 - 101*

98

Novellino., Oliver Werz., Pietro Campiglia., Giuseppe Bifulco. (2017). Identification of novel microsomal prostaglandin E 2 synthase-1 (mPGES-1) lead inhibitors from Fragment Virtual Screening. European Journal of Medicinal Chemistry, 125, 278-287. doi:10.1016/j.ejmech.2016.09.042.

33. Filip Bergqvist., Elena Ossipova., Helena Idborg., Joan Raouf., Antonio Checa., Karin Englund., Petter Englund., Payam Emami Khoonsari., Kim Kultima., Craig E., Wheelock., Karin Larsson., Marina Korotkova & Per-Johan Jakobsson. (2019). Inhibition of mPGES-1 or COX-2 Results in Different Proteomic and Lipidomic Profiles in A549 Lung Cancer Cells. Front pharmacol, doi:10.3389/fphar.2019.00636.

34. Maria G. Chini., Assunta Giordano., Marianna Potenza., Stefania Terracciano., Katrin Fischer., Maria C. Vaccaro., Ester Colarusso., Ines Bruno., Raffaele Riccio., Andreas Koeberle., Oliver Werz., Giuseppe Bifulco. (2020). Targeting mPGES-1 by a Combinatorial Approach: Identification of the Amino benzothiazole Scaffold to Suppress PGE 2 Levels. Medicinal chemistry letters, 11, 783-789. doi:10.1021/acsmedchemlett.9b00618.

35. Antonina V. Kurtova., Jing Xiao., Qianxing Mo., Senthil Pazhanisamy., Ross Krasnow., Seth P. Lerner., Fengju Chen., Terrence T. Roh., Erica Lay., Philip Levy Ho & Keith Syson Chan. (2015). Blocking PGE_2-induced tumour repopulation abrogates bladder cancer chemoresistance. Nature, 517, 209-213. doi:10.1038/nature14034

36. Weizhou Hou., Padma Sampath., Juan J.Rojas., Steve H.Thorne. (2016). Oncolytic Virus-Mediated Targeting of PGE_2 in the Tumor Alters the Immune Status and Sensitizes Established and Resistant Tumors to Immunotherapy. Cancer Cell, 30, 108–119. doi:10.1016/j. ccell.2016.05.012.

37. Marc Hennequart., Luc Pilotte., Stefania Cane., Delia Hoffmann., Vincent Stroobant., Etienne De Plaen., Benoît J. Van den Eynde. (2017). Constitutive IDO1 Expression in Human Tumors Is Driven by Cyclooxygenase-2 and Mediates Intrinsic Immune Resistance. Cancer Immunol Res, 5(8), 695–709. doi:10.1158/2326-6066.CIR-16-0400.

38. Kenneth V. Honn., Darryl C. Zeldin. (2019). Advances in Experimental Medicine and Biology, 1161, doi:10.1007/978-3-030-21735-8_1.

39. Sunhwan Jo., Taehoon Kim., Vidyashankara G Iyer., Wonpil Im. (2008). CHARMM-GUI: a web-based graphical user interface for CHARMM. J Comput Chem, 29 (11), 1859-65. doi: 10.1002/jcc.20945.

40. Jumin Lee., Xi Cheng., Jason M. Swails., Min Sun Yeom., Peter K. Eastman.,Justin A. Lemkul., Shuai Wei., Joshua Buckner., Jong Cheol Jeong., Yifei Qi., Sunhwan Jo., Vijay S. Pande., David A. Case., Charles L. Brooks., III, Alexander D. MacKerell, Jr., Jeffery B. Klauda, and Wonpil Im. (2016). J Chem Theory Comput. CHARMM-GUI Input Generator for NAMD, GROMACS, AMBER, OpenMM, and CHARMM/OpenMM Simulations Using the CHARMM36 Additive Force Field, 12 (1), 405-13.doi.org/10.1021/acs.jctc.5b00935 41.Jing Huang., Sarah Rauscher., Grzegorz Nawrocki., Ting Ran., Michael Feig., Bert L de Groot., Helmut Grubmüller., Alexander D MacKerell Jr. (2017). CHARMM36m: an improved force field for folded and intrinsically disordered proteins. Nat Methods, 14 (1), 71-73. doi.org/10.1038/nmeth.4067

42. Tom Darden., Darrin York., Lee Pedersen. (1993). Particle mesh Ewald: An N· log (N) method for Ewald sums in large systems. The Journal of chemical physics, 98 (12), 10089-10092. doi.org/10.1063/1.464397

43. W Humphrey., A Dalke., K Schulten. (1996). VMD: visual molecular dynamics. J Mol Graph, 14 (1), 33-8, 27-8. doi.10.1016/0263-7855(96)00018-5

44. Markus Kuschak., Vigneshwaran Namasivayam., Muhammad Rafehi., Jan H. Voss., Jaspal Garg., Jonathan G. Schlegel, Aliaa Abdelrahman, Stefan Kehraus,Raphael Reher, Jim Küppers, Katharina Sylvester, Sonja Hinz, Michaela Matthey, Daniela Wenzel,Bernd K. Fleischmann, Alexander Pfeifer, Asuka Inoue, Michael Gütschow,Gabriele M. König,Christa E. Müller. (2020). Cell-permeable high-affinity tracers for Gq proteins provide structural insights, reveal distinct binding kinetics and identify small molecule inhibitors. British journal of pharmacology. 177(8), 1898-1916.

45. https://pubs.acs.org/doi/10.1021/jp304056p

46.Wang S., Yang S., An B., Wang S., Yin Y., Lu Y., Xu Y., Hao D. (2011). Molecular Dynamics Analysis Reveals Structural Insights into Mechanism of Nicotine N-Demethylation Catalyzed by Tobacco Cytochrome P450 Mono-Oxygenase. PLoS ONE, 6(8): e23342. doi:10.1371/journal.pone.0023342

47. Krishnendu Bera., V. S. Jeba Reeda., P. R. Babila., Dhurvas Chandrasekaran Dinesh., Jozef Hritz & T. Karthick., (2021). An in silico molecular dynamics simulation study on

Eur. Chem. Bull. **2023**, *12(Issue 9), 82 - 101*

99

the inhibitors of SARS-CoV-2 proteases (3CLpro and PLpro) to combat COVID-19, Molecular Simulation, 47:14, 1168-1184. doi: 10.1080/08927022.2021.1957884

48. Gopinath P. and Kathiravan M. K. (2021). Docking studies and molecular dynamics simulation of triazole benzene sulfonamide derivatives with human carbonic anhydrase IX inhibition activity. RSC Adv,11, 38079-38093. doi.org/10.1039/D1RA07377J

49. https://www.clinicaltrials.gov/ct2/show/NCT0 1632579

50. John Gately Luz., Stephen Antonysamy., Steven L. Kuklish., Bradley Condon., Matthew R. Lee., Dagart Allison., Xiao-Peng Yu., Srinivasan Chandrasekhar., Ryan Backer., Aiping Zhang., Marijane Russell., Shawn S. Chang., Anita Harvey., Ashley V. Sloan., and Matthew J. Fisher (2015). Crystal Structures of mPGES-1 Inhibitor Complexes Form a Basis for the Rational Design of Potent Analgesic and Anti-Inflammatory Therapeutics. Journal of Medicinal Chemistry, 58 (11), 4727-4737. doi.org/10.1021/acs.jmedchem.5b00330

51. Jin Y., Smith CL., Hu L., Campanale KM., Stoltz R., Huffman LG Jr., McNearney TA., Yang XY., Ackermann BL., Dean R., Regev A., Landschulz W. (2016). Pharmacodynamic comparison of LY3023703, a novel microsomal prostaglandin e synthase 1 inhibitor, with celecoxib. Clinical Pharmacology & Therapeutics, 99, 274-84, doi:10.1002/cpt.260.

52. Molecular Operating Environment (MOE), 2018.01, Chemical Computing Group ULC, 1010 Sherbooke St. West, Suite #910, Montreal, QC, Canada, H3A 2R7, 2018.

53. M Rarey., & JS Dixon. (1998). Feature trees: a new molecular similarity measure based on tree matching. Journal of Computer Aided Molecular Design,12(5), 471-490.

54. Matthias Rarey & Martin Stahl. (2001). Similarity searching in large combinatorial chemistry spaces. Journal of Computer Aided Molecular Design, 15, 497-520. doi:10.1023/a:1011144622059.

55. Daigen Xu., Steven E. Rowland., Patsy Clark., André Giroux., Bernard Côté., Sébastien Guiral., Myriam Salem, Yves Ducharme., Richard W. Friesen., Nathalie Méthot., Joseph Mancini., Laurent Audoly and Denis Riendeau. (2008). MF63 [2-(6-Chloro-1H-phenanthro [9,10-d]imidazol-2-yl)-isophthalonitrile], a Selective Microsomal Prostaglandin E Synthase-1 Inhibitor, Relieves Pyresis and Pain in Preclinical Models of Inflammation. Journal of Pharmacology and Experimental Therapeutics, 326 (3), 754-763, doi:10.1124/jpet.108.138776.

56. Andreas Koeberle., Antonietta Rossi., Heiko Zettl., Carlo Pergola., Friederike Dehm., Julia Bauer., Christine Greiner., Sina Reckel., Christina Hoernig., Hinnak Northoff., Frank Bernhard., Volker Dötsch., Lidia Sautebin., Manfred Schubert Zsilavecz and Oliver Werz. (2010). The Molecular Pharmacology and In Vivo Activity of 2-(4-Chloro-6-(2,3-dimethylphenylamino) pyrimidin-2-ylthio)octanoic acid (YS121), a Dual Inhibitor of Microsomal Prostaglandin E2 Synthase-1 and 5-Lipoxygenase. Journal of Pharmacology and Experimental Therapeutics, 332 (3), 840-848, doi:10.1124/jpet.109.160663.

57. KijaeLee., Van Chung Pham., Min Ji Choi., Kyung Ju Kim., Kyung-TaeLee., Seong-Gu Han., Yeon Gyu Yu., Jae Yeol Leea. (2013). Fragment-based discovery of novel and selective mPGES-1 inhibitors Part 1: Identification of sulfonamido-1,2,3-triazole-4,5-dicarboxylic acid. Bioorganic & Medicinal Chemistry Letters, 23(1), 75-80, doi:10.1016/j.bmcl.2012.11.019.

58. Sung-Jun Park., Seong-Gu Han., Hafiz Muhammad Ahsan., Kijae Lee., Jae Yeol Lee., Ji-Sun Shin., Kyung-Tae Lee., Nam-Suk Kang., Yeon Gyu Yua. (2012). Identification of novel mPGES-1 inhibitors through screening of a chemical library. Bioorganic & Medicinal Chemistry Letters, 24(15), 7335-7339, doi:10.1016/j.bmcl.2012.10.085.

59. Daniel P. Walker., Graciela B. Arhancet., Hwang-Fun Lu., Steven E. Heasley., Sue Metz., Natasha M. Kablaoui., Francisco M. Franco., Cathleen E.Hanau., Jeffrey A. Scholten., John R. Springer., Yvette M. Fobian., Jeffrey S.Carter., Li Xing., Shengtian Yang., Alexander F. Shaffer., Gina M. Jerome., Michael T. Baratta., William M.Moore., Michael L.Vazquez. (2013). Synthesis and biological evaluation of substituted benzoxazoles as inhibitors of mPGES-1: Use of a conformation-based hypothesis to facilitate compound design. Bioorganic & Medicinal Chemistry Letters, 23 (14), 1120-126, doi:10.1016/j.bmcl.2012.11.107.

60. Verhoff M., Seitz S, Paul M, Noha SM, Jauch J, Schuster D, Werz O. (2014). Tetra- and Pentacyclic Triterpene Acids from the Ancient Anti-inflammatory Remedy Frankincense as Inhibitors of Microsomal Prostaglandin E2 Synthase-1. Journal of Natural Products, 77, 1445-1451, doi:10.1021/np500198g.

Eur. Chem. Bull. **2023**, *12(Issue 9), 82 - 101*

100

61. Chandrasekhar S., Harvey AK., Yu XP., Chambers MG., Oskins JL., Lin C., Seng TW., Thibodeaux SJ., Norman BH., Hughes NE., Schiffler MA., Fisher MJ. (2016). Identification and Characterization of Novel Microsomal Prostaglandin E Synthase-1 Inhibitors for Analgesia. Journal of Pharmacology and Experimental Therapeutics, 356(3), 635-644, doi:/10.1124/jpet.115.228932.
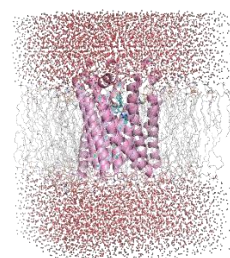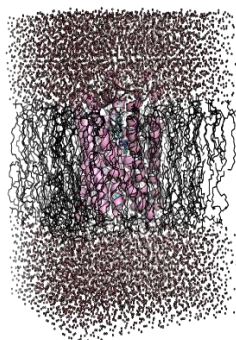
Supplementary

Fig.S1: Ligand PV-001857177657 inside the binding pocket of PDB Id: 4YL1 identified from the docking study
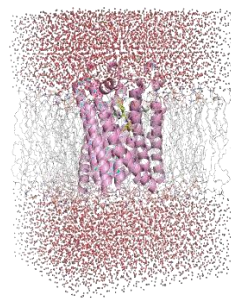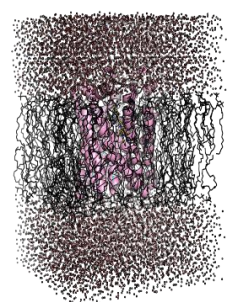

Fig.S2: Ligand PV-002331049037 inside the binding pocket of PDB Id: 4YL1 identified from the docking study
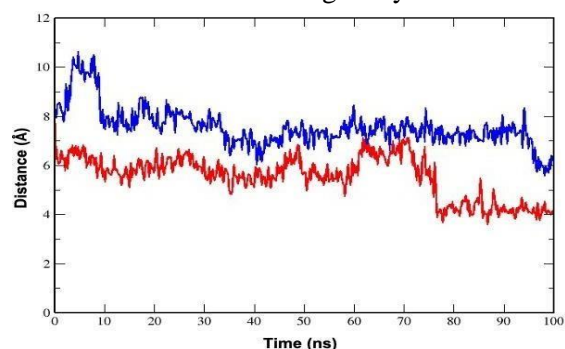

Fig.S3: PV-001857177657(red), PV-002331 04 9037(blue) and the cofactor GSH is calculated from the trajectories for a period of 100 ns molecular dynamics simulations.

Table S1: The Hydrogen Bond Occupancy Of Each Interacting Residue In Their Respective Ligand In The Complexes With Mpges Over 100 Ns Trajectory

Donor	Acceptor	Occupancy
Lig01-Side	THR131-Side	9.78%
Lig01-Side	GLY35-Main	0.80%
Lig01-Side	GLN36-Side	0.40%
Lig01-Side	HSD53-Side	0.80%
Lig01-Side	ILE32-Side	0.20%
GLN36-Side	Lig01-Side	1.40%
PHE44-Side	Lig01-Side	0.20%
Donor	**Acceptor**	**Occupancy**
PHE44-Side	Lig02-Side	0.20%
THR131-Side	Lig02-Side	3.59%
GLN36-Side	Lig02-Side	0.20%
GLN134-Side	Lig02-Side	2.79%
SER127-Side	Lig02-Side	5.79%
Lig02-Side	THR131-Side	2.20%
ASP49-Main	Lig02-Side	2.20%
ALA123-Side	Lig02-Side	0.60%
ARG52-Side	Lig02-Side	0.60%
Lig02-Side	HSD53-Side	0.20%
Lig02-Side	SER127-Side	0.20%

Eur. Chem. Bull. **2023**, *12(Issue 9), 82 - 101*

101